https://doi.org/10.20965/ijat.2023.p0610

Research Paper:

Detection of Multiscale Deterioration from Point-Clouds of Furnace Walls

Tomoko Aoki, Erika Yamamoto, and Hiroshi Masuda[†]

The University of Electro-Communications
1-5-1 Chofugaoka, Chofu, Tokyo 182-8585, Japan
[†]Corresponding author, E-mail: h.masuda@uec.ac.jp
[Received March 30, 2023; accepted August 18, 2023]

Deterioration surveys of large structures such as furnaces have been mainly conducted by visual inspection, but it is desirable to automatically detect deterioration using point clouds captured by the terrestrial laser scanner. In this study, we propose flexible methods for detecting various scales of cracks, delamination, and adhesion on furnace walls by using a machine learning technique. Since small cracks have few geometrical features, they are detected from the reflection intensity images generated by projecting a point cloud onto a two-dimensional plane. For detecting cracks on the image, we use the U-Net fine-tuned by crack images denoised with a median filter. For detecting delamination and adhesion, a wall surface is approximated by a smooth B-spline surface, and deterioration is detected as differences between the point cloud and the approximated surface. However, in this method, the resolution of the B-spline surface has to be carefully determined according to the expected deterioration sizes. To robustly detect deterioration at various scales, we introduce multiscale 3D features, and detect deterioration using both multiscale 3D features and 2D features. In actual walls, it is difficult to distinguish between cracks and delamination because delamination grows from cracks. To detect both types of deterioration in a uniform manner, we combine the two detectors and propose an integrated detector for detecting deterioration at various scales. Our experimental results showed that our methods could stably detect various scales of degradation on furnace walls.

Keywords: terrestrial laser scanner, point cloud, point processing, deterioration detection, machine learning

1. Introduction

While industrial facilities built during Japan's economic growth period are in need of maintenance, a lack of human resources makes labor-intensive maintenance work difficult. To improve the efficiency of maintenance work, point clouds captured by a terrestrial laser scanner (TLS) are effective. By utilizing high-density point clouds of an industrial facility, the current status of the facility can be acquired and inspected. For example, Kitratporn et al. [1] measured deformations such as tilt and deflection in bridges using point clouds. Hada et al. [2] developed a bridge inspection system using point clouds acquired by a bridge inspection support robot.

In recent years, the accuracy and density of point clouds have greatly improved, and point clouds can now be used to detect deterioration at various scales. Traditionally, deterioration of large-scale facilities has been diagnosed mainly by visual inspection, but the quality of visual inspection is often dependent on the skills of operators. Furthermore, it is difficult to quantitatively measure deterioration by visual inspection. If point clouds can be used to detect the location and extent of deterioration, it is expected to improve the efficiency and quality of inspections of facilities.

In this paper, we discuss methods for stably detecting delamination, adhesion, and cracks from point clouds of walls of large facilities. While many existing methods have been proposed to detect deterioration on flat planar walls, we consider walls with rotational shapes, such as blast furnaces and storage tanks.

Since the actual wall shapes often differ from the shapes specified in the drawings, it is required to distinguish deterioration from distortion caused by the construction process. In addition, deterioration detection requires careful parameter tuning depending on the scale of deterioration. We eliminate such trial-and-error parameter tuning by using a machine learning technique [3].

We note that the methods discussed in this paper will be applicable to various facilities with rotating shapes, but we focus on deterioration detection for furnace walls because deterioration detectors require training data for machine learning, which depend on the deterioration modes for each facility type.

First, we discuss methods for detecting delamination and adhesion with relatively large scales. For adhesion and delamination, we extend the method proposed by Shinozaki et al. [4, 5] and introduce a new detector using multiscale 3D features combined with 2D features. While the method in [4, 5] required careful parameter tuning according to the scales of deterioration, our method does not need such trial-and-error parameter tuning by using machine learning techniques. Next, we discuss methods for detecting cracks with smaller scales. For crack detection,

we improve the method proposed by Yamamoto et al. [6]. Finally, we propose an integrated method for detecting all of delamination, adhesion, and crack in a uniform manner. In actual walls of large facilities, delamination often occurs due to the crack growth. It is difficult to distinguish between delamination and cracks due to many intermediate cases. Therefore, we unify the two detectors to detect delamination, adhesion, and cracks in a unified manner.

Section 2 describes the related work, and Section 3 outlines our proposed methods. Section 4 describes the method for detecting delamination and adhesion, and Section 5 describes the method for detecting cracks. Then, Section 6 describes the integrated deterioration detection method. Section 7 presents the experimental results, and finally, we conclude the paper in Section 8.

2. Related Work

2.1. Deterioration Detection from Point Cloud

In typical methods for detecting deterioration from point clouds, a wall surface with no deterioration is used as a reference surface, and the difference between the reference surface and a point cloud is detected as deterioration. However, there are many cases where drawings are not available for old facilities, or where the drawings differ from the actual conditions. In such cases, an estimation of the reference surface is necessary.

For planar reference surfaces, many methods have been studied. Zhang et al. [7] proposed a method for detecting deterioration based on the difference between a point cloud and the reference contours obtained from drawings of reinforced concrete columns. Mizoguchi et al. [8] detected delamination on planar walls of bridges from a time series of point clouds. Their method estimated the healthy surfaces from point clouds measured at different times, aligned the point clouds, and detected the time-series growth of delamination. Nespeca and De Luca [9] detected deterioration by using the photogrammetrically estimated planes as the reference plane. Seo et al. [10] detected deterioration by extracting cross sections from point clouds and comparing them with the cross sections specified in the drawings. Some researchers have detected deterioration of cylindrical walls. Wu et al. [11] assumed the reference surface to be a cylinder and detected degradation using the ratio of the surface areas of a point cloud and the reference surface.

These methods assume that the wall surface was constructed exactly as a plane or cylinder. However, walls with rotational shapes, such as blast furnaces and storage tanks, are often not constructed exactly as specified in the drawings, and the actual walls often contain undulations and distortions caused by the construction process. In such cases, assuming that the reference surface is an exact plane or cylinder may lead to misidentification of distortion during construction as deterioration.

Shinozaki et al. [4] assumed that the wall surface constructed as a rotational surface was a smooth surface at the time of construction, rather than assuming it to be an exact rotational surface. In this method, a B-spline surface is fitted to a point cloud, and the difference between the point cloud and the B-spline surface is considered to be delamination or adhesion. They controlled the scale of detectable deterioration by increasing or decreasing the number of control points of the B-spline surface. However, in this method, the appropriate number of control points must be determined experimentally by trial and error. They further tried to detect small cracks by increasing the number of control points [5]. However, crack detection requires very dense point clouds, and it is difficult for large facilities to acquire dense point clouds at a distance from the scanner.

In this paper, we extend the method proposed by Shinozaki et al. [4, 5] by using multi-resolution B-spline surfaces. In our method, parameters for deterioration detection are automatically selected by random forests [3]. Furthermore, we improve the detection performance by combining multiscale 3D features with 2D features.

2.2. Deterioration Detection from 2D Image

While delamination and adhesion can be detected as displacement from the reference surface, cracks are too small to be detected stably as displacement. Therefore, different methods are required for crack detection. One promising approach is to generate 2D images from a point cloud and solve the crack detection problem from the images. A dense point cloud acquired by a TLS can be projected onto a 2D plane to create an image. The reflection intensity or RGB of each point is used as the pixel value in the image. The reflection intensity value is calculated from the intensity of the reflected laser beam and is output from a typical laser scanner as an attribute of each point.

Deterioration detection from images has been studied extensively. There are two main types of methods: classical image processing methods and deep learning methods.

In image processing methods, cracks are typically detected by extracting edges using image filters and thresholding. O'Byrne et al. [12] detected edges in a histogram-flattened HDR image and segmented degraded areas. Dapiton et al. [13] proposed a method for detecting deterioration on wall surfaces by combining pre-processing and edge extraction.

A large number of deep learning methods based on convolutional neural networks (CNN) have been proposed. In these methods, CNNs are trained using a large number of images to detect and extract various objects from images. Cracks can be detected by training a CNN using crack images. For example, Cha et al. [14] showed that CNNs can be used to detect deterioration without being affected by light or shadow.

Yamamoto et al. [6] showed that the reflectance intensity of a point cloud is useful for detecting cracks. At cracks, the reflection intensity significantly changes due to the sudden change in the angle of laser irradiation to the wall surface. They detected cracks from the reflection intensity images using U-Net [15], which was trained us-

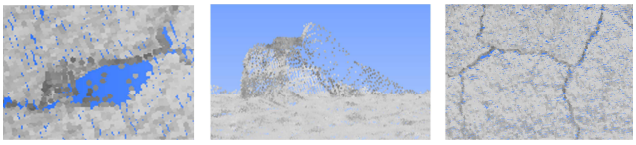

(a) Delamination (b) Adhesion (c) Crack

Fig. 1. Deterioration types.

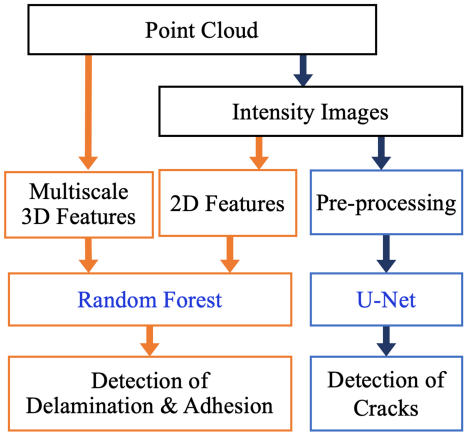

Fig. 2. Two detectors for large-scale and small-scale deterioration.

ing crack images. However, this method could not achieve a sufficiently high detection rate of about 50%.

In this paper, we improve the method proposed by Yamamoto et al. [6] to increase the accuracy of crack detection from reflection intensity images. Furthermore, we detect deterioration at various scales without distinguishing between cracks and delamination.

3. Overview

Deterioration of wall surfaces is classified into delamination, adhesion, and cracks, as shown in **Fig. 1**.

Figure 2 shows the process of detecting deterioration. This method uses different detectors to detect delamination or adhesion, where the scale is relatively large, and cracks, where the scale is small. In machine learning, random forests are used for detecting delamination and adhesion, and U-Net is used for detecting cracks.

In our method, a reflection intensity image is generated from a point cloud and is used for deterioration detection. In this paper, the reflection intensity image is simply denoted as intensity image.

In **Fig. 3**, the two detectors are integrated to detect adhesion, delamination, and cracks in a unified manner. In the integrated detector, the output of the crack detector is used as the input to random forests.

3.1. Delamination and Adhesion Detector

The detector for delamination and adhesion is shown on the left side of **Fig. 2**.

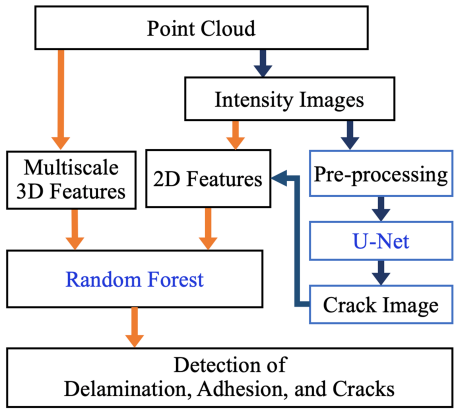

Fig. 3. Integrated detector to detect deterioration at various scales.

To avoid trial-and-error parameter tuning, 3D features are calculated from the point cloud in a multiscale manner. The required scales of features are automatically selected from the multiscale features using random forests, which is a commonly used supervised machine learning method consisting of multiple decision trees [3].

The 3D features include the difference from the B-spline surface, and the flatness and curvature calculated using neighbor points. The difference feature is calculated as the difference between the point cloud and the B-spline surface fitted to a point cloud. Multiscale difference values are obtained from B-spline surfaces computed with different numbers of control points. For flatness and curvature, multiscale features are computed by changing the neighborhood radius.

The reflection intensity at each point is also useful to detect deterioration. In our method, the reflection intensity and the edge-enhanced reflection intensity are optionally used as 2D features. Then, both multiscale 3D features and 2D features are input to random forests to detect deterioration.

3.2. Crack Detector

The crack detection procedure is shown on the right side of **Fig. 2**. In our method, cracks are detected from the intensity image generated from the point cloud.

For crack detection, we use a U-Net which is fine-tuned using crack images. The U-Net is a deep learning model for image segmentation [15]. In our previous work [6], crack detection based on U-Net could not achieve a high detection rate. In this paper, we show that pre-processing of intensity images is important to improve the crack detection using U-Net.

3.3. Integrated Deterioration Detector

The output of U-Net is a crack image. To integrate the crack detector with the delamination and adhesion detector, the crack image generated by the U-Net is added to the 2D features, as shown in **Fig. 3**. Then, the integrated features are input to random forests for detecting delamination, adhesion, and cracks in a unified manner.

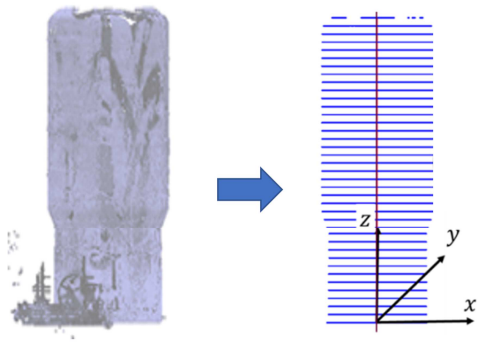

(a) Estimation of the center axis from point clouds

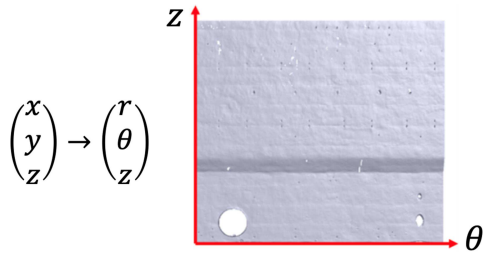

(b) Translation to cylindrical coordinates

Fig. 4. Mapping points onto the θ–z plane.

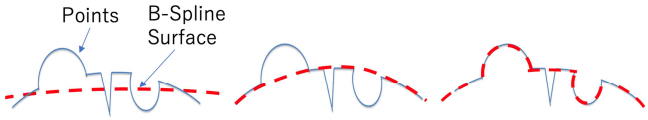

(a) Low resolution (b) Middle resolution (c) High resolution

Fig. 5. Multiscale differences calculated using B-spline surfaces with difference numbers of control points.

4. Detection of Delamination and Adhesion

As 3D features, the difference from the reference surface, flatness, and curvature are used. The 3D features are calculated at multiple scales so that deterioration at various scales can be stably detected.

This research targets the detection of deterioration of walls with rotational shapes. As shown in **Fig. 4(a)**, a rotational surface can be represented using the cylindrical coordinate system with the z-axis as the central axis, r as the radial direction, and θ as the circumferential direction. The central axis can be obtained as a straight line passing through the centers of the circular section points in the height direction [4].

The points on the rotational surface are approximated by a B-spline surface parameterized by z and θ in cylindrical coordinates, as shown in **Fig. 4(b)**. The differences are calculated by using the B-spline surface as the reference surface. As shown in **Fig. 5**, a B-spline surface with a small number of control points is used to detect large-scale deterioration, while a surface with a large number of control points is used to detect small-scale deterioration. To obtain multiscale 3D difference features, B-spline surfaces are computed using various numbers of control points.

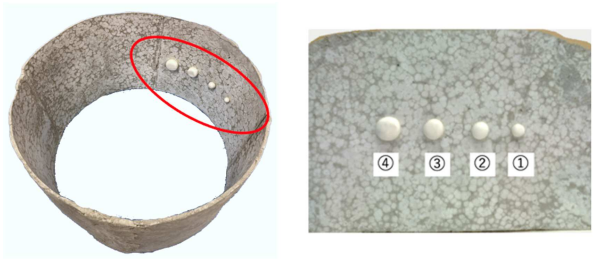

Fig. 6. Sample wall with adhering substances.

Table 1. Sizes of adhesions.

	1	2	3	4
Diameter	10 mm	15 mm	20 mm	25 mm
Thickness	5 mm	7.5 mm	10 mm	12.5 mm

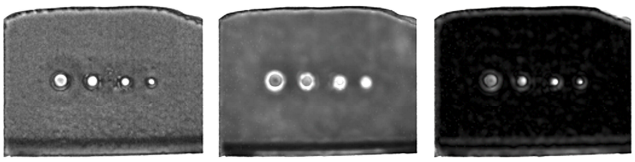

(a) Difference (b) Flatness (c) Curvature

Fig. 7. 3D features calculated from a point cloud.

The flatness and curvature features are computed at each point using eigenvalues obtained by applying principal component analysis to the neighbor points. When eigenvalues are denoted as λ_1, λ_2, and λ_3 ($\lambda_1 \geq \lambda_2 \geq \lambda_3$), the flatness feature is calculated as the minimum eigenvalue λ_3 and the curvature feature as $\lambda_3/(\lambda_1+\lambda_2+\lambda_3)$. In order to calculate multiscale features, the flatness and curvature features are calculated using multiple neighborhood distances for neighbor points.

Figure 6 shows a cylindrical cement wall model with various sizes of adhesions. The sizes of adhesions are shown in **Table 1**. We captured a point cloud of this model using a TLS, and calculated 3D features from the point cloud. **Fig. 7** shows the difference, flatness, and curvature features.

Intensity images would also be effective in detecting deterioration because the reflection intensity changes significantly at the location of degradation, as shown in **Fig. 8**. In our method, 2D features calculated from intensity images can be optionally added to the random forests input. The edge-enhanced intensity value is calculated by applying the Canny filter to the intensity image denoised with a median filter. In this paper, we use two types of median filters. One is a typical 5×5 median filter, which prevents the salt-and-pepper noise generated by missing points from being detected as edges. The other is a median filter that finds the median from the neighbor pixels other than the missing points. This filter prevents valid points from being removed as noise, especially when many neighbor points are missing at positions

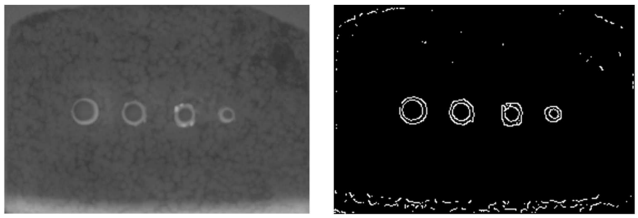

(a) Intensity image (b) Edge-enhanced image

Fig. 8. 2D features obtained from intensity image.

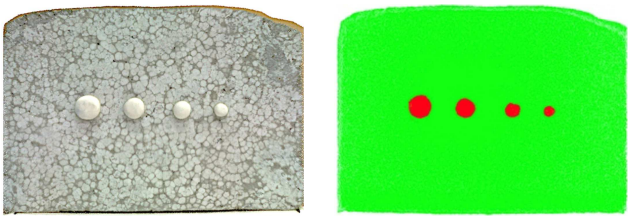

(a) Camera image (b) Ground-truth

Fig. 9. The ground-truth of adhesions.

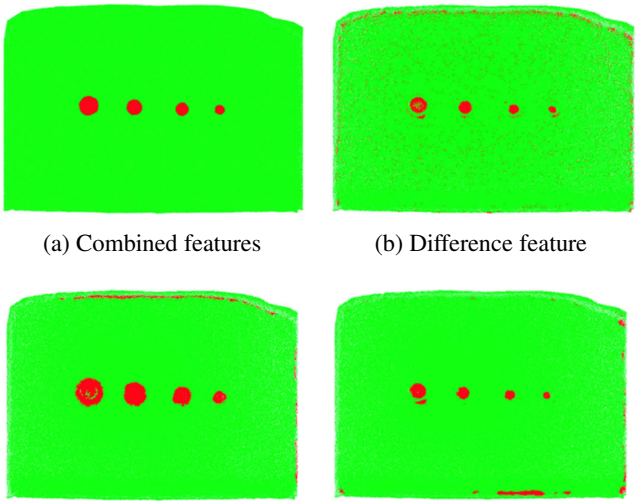

(a) Combined features (b) Difference feature

(c) Flatness feature (d) Curvature feature

Fig. 10. Adhesions detection using random forests.

far from the scanner. In our method, each point has two edge-enhanced intensity values computed using two types of median filters.

3D multi-scale features and optionally 2D features are computed at each point and they are input to random forests. The random forests are trained using the ground-truth training data to determine whether each point is deterioration or not.

Figure 9 shows the ground-truth image of adhesions, which was manually created. **Fig. 10** shows regions detected as deterioration using 3D multiscale features. Although each of the difference, flatness, and curvature features produced many false positive results for degradation, the combination of all 3D features could correctly detect deterioration regions.

In our method, many features are input in a multiscale manner, and random forests automatically select only effective features according to the training data. We will discuss which of the input features are effective in a later section.

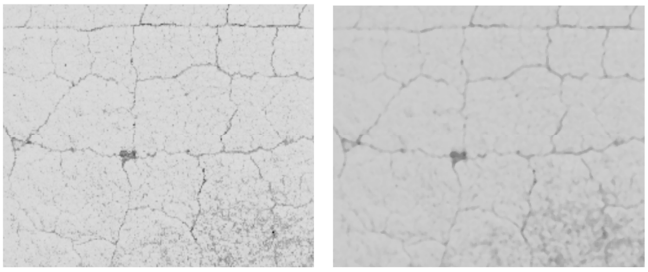

(a) Original intensity image (b) Median filtered image

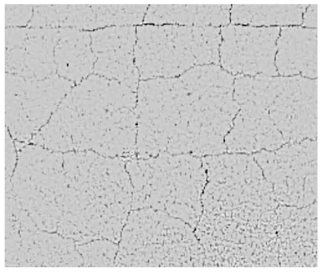

(c) Pre-processed image

Fig. 11. Pre-processed intensity image.

5. Crack Detection from Intensity Image

In our previous work [6], a U-Net model pre-trained using ImageNet was used for crack detection. We fine-tuned the pre-trained model using 9,603 RGB images of cracks, which were used in other crack detection researches [16–20]. However, in our experiments, this fine-tuned U-Net model could not achieve a high crack detection rate when applied to intensity images generated from point clouds.

We consider that there are two possible reasons for this problem: (1) the cracks could not be detected due to stains and color irregularities on the wall surfaces, and (2) since the pixels of cracks tend to be discontinuous in the intensity image generated from a point cloud, the U-Net trained using camera images did not adapt to the cracks in the intensity images.

To solve these problems, the intensity image is pre-processed to remove noise such as color irregularities. In addition, U-Net is further fine-tuned using intensity images generated from point clouds.

Let I_o be the original intensity image, I_m be the image obtained by applying a 5×5 median filter to I_o, and $I_o(i, j)$ and $I_m(i, j)$ be the pixel values at (i, j). As shown in **Fig. 11(b)**, by applying the median filter to the intensity image, discrete crack pixels are smoothed and blurred, but stains and color irregularities tend to remain unchanged. Therefore, stains and color irregularities are reduced and cracks are sharpened by applying the following equation

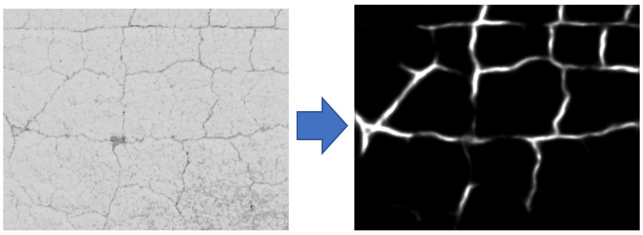

(a) Previous method [6]

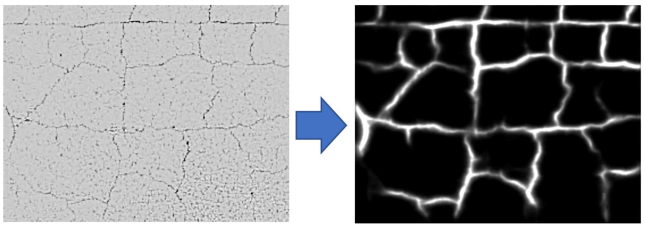

(b) Our method

Fig. 12. Detected cracks from intensity image.

Table 2. Detection rates for cracks.

	Detection rate
Previous method [6]	55%
Our method	91%

to the intensity image.

$$I_n(i,j) = \frac{1}{2} \times \frac{I_o(i,j)}{I_m(i,j)} \times 255. \quad \cdots \quad (1)$$

An example of the result is shown in **Fig. 11(c)**.

To train U-Net to recognize cracks in intensity images, we created a training dataset by extracting cracks from 400 intensity images, which were cropped from point clouds of furnace walls. The training dataset was created by manually drawing line segments on cracks in the intensity images using a drawing tool. The training dataset was used for fine-tuning the U-Net.

Figure 12 shows the cracks detected by our method and the previous method [6]. The detection rates are shown in **Table 2**. In this evaluation, a continuous unbranched line segment was counted as one crack. The detection rate is defined as the ratio of the number of detected cracks to the total number of cracks that can be visually observed. Our method could achieve significantly better detection rates.

6. Integrated Deterioration Detector

In Sections 4 and 5, delamination and cracks are detected using two independent detectors, which have to be trained using different training data. One of the two detectors is suitable for detecting relatively large deterioration such as delamination and adhesion, while the other is suitable for detecting small deterioration such as cracks. This is because the crack detector removes the delaminated area as noise and cannot stably detect delamination

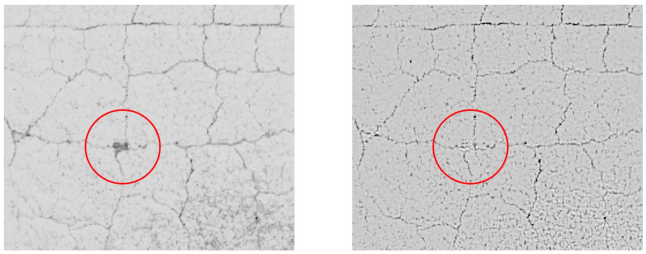

Fig. 13. Disappearance of delamination in the pre-process of crack detection.

Table 3. The numbers of features for the integrated detector.

	Feature type	Number of features
3D features	Difference from reference	10
	Flatness	18
	Curvature	18
2D features	Intensity image	1
	Edge-enhanced image	2
	Crack image	1

as shown in **Fig. 13**. Similarly, small cracks cannot be stably detected using the detector for delamination and adhesion.

However, in actual wall surfaces, delamination often grows gradually from cracks, and it is difficult to strictly distinguish between cracks and delamination. Therefore, we introduce an integrated detector for all of delamination, adhesion, and cracks.

Since the crack detector detects the pixels of cracks in the intensity image, the output of the crack detector can be regarded as a 2D feature of each point, as shown in **Fig. 3**. By adding the output of the crack detector to the input of the random forests, features for delamination, adhesion, and cracks can be integrated. In the integrated detector, the 2D features consist of an intensity image, two edge-detected images, and a crack image.

In the integrated detector, the differences from the reference surfaces are computed using B-spline surfaces with different numbers of control points. For multiscale difference features, any combinations of resolutions can be selected for B-spline surfaces, depending on the scales of deterioration to be detected. In this paper, control points in the u- and v-directions are selected in 10 different resolutions, which include 10×10, 13×13, 24×24, 45×45, 10×13, 13×10, 13×24, 24×13, 24×45, and 45×24. Flatness and curvature are also calculated in a multiscale manner by changing the neighborhood distances. In this paper, a total of 18 features are calculated for flatness and curvature using distances every 10 mm from 10 to 100 mm and every 50 mm from 100 to 500 mm, respectively.

Table 3 shows the list of features used for the integrated detector. The feature vector of each point consists of 46 multiscale 3D features and four 2D features for a total of 50 features.

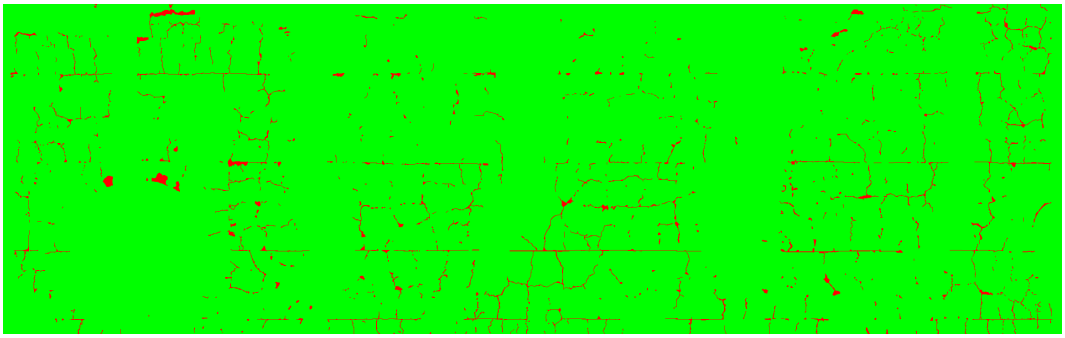

(a) Ground-truth

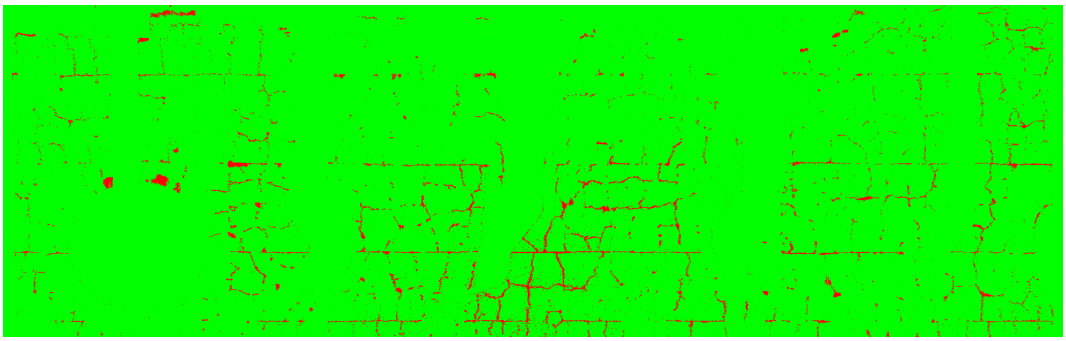

(b) Our method

Fig. 14. Detection of deteriorations on the blast furnace wall.

7. Experimental Results

In our experiments, we used point clouds of a blast furnace measured at 12 locations. The number of points was totally about 450 million. The laser scanner used was Leica ScanStation C10. The point cloud density was 6.3 mm at 10 m, and approximately 40 million points were acquired in a single scan. Since the various equipment was installed inside the furnace, point clouds were acquired at 12 locations using the laser scanner on the floor so that occluded regions on the furnace wall were reduced as much as possible.

To create the ground-truth dataset, we converted each point cloud into an intensity image and manually painted the deteriorated regions red using a painting tool. We note that we used both the intensity image and the 3D rendering of the point cloud to visually find deterioration regions. Finally, we classified each point as either "deteriorated" or "sound" without distinguishing between delamination, adhesion, and cracks. An example of the ground-truth data is shown in **Fig. 14(a)**.

For the integrated detector, 80% of the ground-truth data was used as training data and 20% as test data. After training the integrated detector, deteriorated regions were detected from the test data. **Fig. 14(b)** shows the deteriorated regions detected from the point cloud shown in **Fig. 14(a)**. This result shows that the integrated detector could detect almost the same deterioration as the ground-truth data.

For quantitative evaluation, precision and recall were evaluated by comparing the ground-truth data and the detected deterioration. For the evaluation of precision, the points detected as deteriorated were considered to be correct if there were the ground-truth data within one-neighbor in the intensity image. For the evaluation of recall, the ground-truth points were considered to be detected if deterioration points were detected within one-neighbor. The F-value was also calculated as the harmonic mean of precision and recall. The results are shown in **Table 4**. The F-value of 90% indicates that the integrated detector was able to achieve a very high deterioration detection rate.

Table 4. Detection rate of deteriorations.

	Precision	Recall	F-score
Integrated detector	92%	88%	90%
Multiscale differences	46%	73%	56%

For comparison, deterioration was detected from the same point clouds using the method proposed in [4, 5]. In this method, a B-spline surface was used as a reference surface, and deterioration was detected using the difference between the reference surface and the point cloud. They detected large-scale deterioration and small-scale cracks separately, but we extended their method in a multiscale manner and detected deterioration at various scales using multiscale differences. This is because the original method requires experimental determination of scale parameters depending on the scale of deterioration and

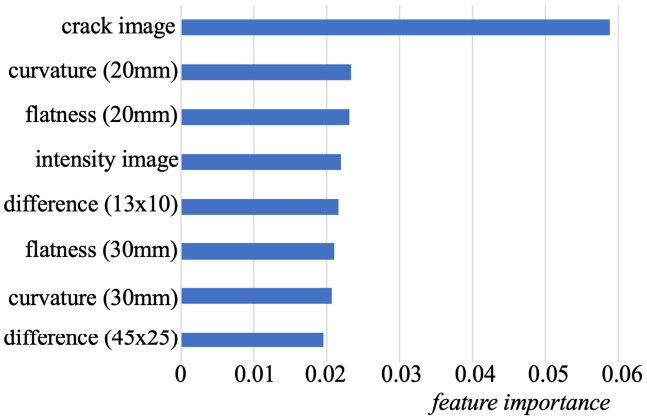

Fig. 15. Ranking of the importance of features.

cannot be compared with the proposed method under the same conditions. Therefore, we introduced multi-scale features to avoid the experimental parameter adjustment.

The result is shown in **Table 4**. The F-value was 56%, and their method could not achieve a high recognition rate. Precision is low at 46%, and this result indicates that a large number of false deterioration points were detected. Compared with this result, our integrated detector could significantly reduce the false-positives and improve the deterioration detection rate.

Random forests can compute the contribution of each feature as feature importance. We calculated feature importance to investigate effective features among the 50 dimensional features of the integrated detector. **Fig. 15** shows the ranking of important features. While the importance of the crack image was very high, the 3D and 2D features also contributed to the detection of deterioration. Our method computed 3D features at various scales without considering the sizes of deterioration, but the integrated detector could automatically select scales of 3D features that were effective in detecting deterioration in the example point clouds.

In summary, the integrated detector has some advantages compared with the methods shown in **Fig. 1**. First, the integrated deterioration detector can achieve very high detection rates compared with conventional methods [4, 5]. The feature importance in **Fig. 15** shows that the integrated detector works effectively by concatenating features from the two detectors. Second, while it is difficult to strictly distinguish between delamination and cracks when creating training data from actual point clouds, the integrated deterioration detector does not require delamination and cracks to be labeled separately.

8. Conclusion

This paper proposed methods for stably detecting delamination, adhesion, and cracks. First, we proposed a method for detecting delamination and adhesion using 3D multiscale features and 2D features. Then, we proposed a method for detecting cracks from pre-processed intensity images using U-Net, which was fine-tuned by intensity images. Finally, we proposed the integrated detector to detect delamination, adhesion, and cracks in a unified manner. We evaluated the integrated detector using point clouds of a blast furnace. Our experimental results showed that our method could successfully detect deterioration on walls.

We believe that our method could be applied to various facilities, such as storage tanks with rotational shapes. We would like to apply our methods to such facilities by investigating their deterioration modes if point clouds are available. Our method requires a lot of training data, but it is time-consuming to create training datasets. We would like to investigate methods to create training data easily or methods to train the detector with less training data.

References:

[1] N. Kitratporn, W. Takeuchi, K. Matsumoto, and K. Nagai, "Structure Deformation Measurement with Terrestrial Laser Scanner at Pathein Bridge in Myanmar," J. Disaster Res., Vol.13, No.1, pp. 40-49, 2018. https://doi.org/10.20965/jdr.2018.p0040
[2] Y. Hada et al., "Development of a Bridge Inspection Support System Using Two-Wheeled Multicopter and 3D Modeling Technology," J. Disaster Res., Vol.12, No.3, pp. 593-606, 2017. https://doi.org/10.20965/jdr.2017.p0593
[3] L. Breiman, "Random Forests," Machine Learning, Vol.45, No.1, pp. 5-32, 2001. https://doi.org/10.1023/A:1010933404324
[4] Y. Shinozaki, K. Kohira, and H. Masuda, "Detection of Deterioration of Furnace Walls Using Large-Scale Point-Clouds," Computer-Aided Design and Applications, Vol.15, No.4, pp. 575-584, 2018. https://doi.org/10.1080/16864360.2017.1419645
[5] Y. Shinozaki and H. Masuda, "Point-Based Virtual Environment for Detecting Scaffolding, Wearing, and Cracks of Furnace Walls," Proc. of ASME 2018 Int. Design Engineering Technical Conf. and Computers and Information in Engineering, DETC2018-85696, 2018. https://doi.org/10.1115/DETC2018-85696
[6] E. Yamamoto, I. Yoshiuchi, and H. Masuda, "Deterioration Detection for Wall Surfaces of Large-Scale Structure Using Dense Point Cloud," 18th Int. Conf. on Precision Engineering (ICPE2020), D-5-5, 2020.
[7] H. Zhang, Y. Zou, E. d. R. Castillo, and X. Yang, "Detection of RC Spalling Damage and Quantification of its Key Properties from 3D Point Cloud," KSCE J. of Civil Engineering, Vol.26, No.5, pp. 2023-2035, 2022. https://doi.org/10.1007/s12205-022-0890-y
[8] T. Mizoguchi et al., "Quantitative Scaling Evaluation of Concrete Structures Based on Terrestrial Laser Scanning," Automation in Construction, Vol.35, pp. 263-274, 2013. https://doi.org/10.1016/j.autcon.2013.05.022
[9] R. Nespeca and L. De Luca, "Analysis, Thematic Maps and Data Mining from Point Cloud to Ontology for Software Development," The Int. Archives of the Photogrammetry, Remote Sensing and Spatial Information Sciences, Vol.XLI-B5, pp. 347-354, 2016. https://doi.org/10.5194/isprs-archives-XLI-B5-347-2016
[10] D.-J. Seo, J. C. Lee, Y.-D. Lee, Y.-H. Lee, and D.-Y. Mun, "Development of Cross Section Management System in Tunnel Using Terrestrial Laser Scanning Technique," The Int. Archives of the Photogrammetry, Remote Sensing and Spatial Information Sciences, Vol.XXXVII-B5, pp. 573-581, 2008.
[11] H. Wu et al., "Concrete Spalling Detection for Metro Tunnel from Point Cloud Based on Roughness Descriptor," J. of Sensors, Vol.2019, 8574750, 2019. https://doi.org/10.1155/2019/8574750
[12] M. O'Byrne, B. Ghosh, F. Schoefs, and V. Pakrashi, "Regionally Enhanced Multiphase Segmentation Technique for Damaged Surfaces," Computer-Aided Civil and Infrastructure Engineering, Vol.29, No.9, pp. 644-658, 2014. https://doi.org/10.1111/mice.12098
[13] R. M. Dapiton, J. R. P. Gonzaga, and R. G. Garcia, "Determination of Unsound Concrete Using Non-Destructive Testing in a Smooth Concrete Through Various Image Processing Techniques," 2021 IEEE 13th Int. Conf. on Humanoid, Nanotechnology, Information Technology, Communication and Control, Environment, and Management (HNICEM), 2021. https://doi.org/10.1109/HNICEM54116.2021.9731921
[14] Y.-J. Cha, W. Choi, and O. Büyüköztürk, "Deep Learning-Based Crack Damage Detection Using Convolutional Neural Networks," Computer-Aided Civil and Infrastructure Engineering, Vol.32, No.5, pp. 361-378, 2017. https://doi.org/10.1111/mice.12263

[15] O. Ronneberger, P. Fischer, and T. Brox, "U-Net: Convolutional Networks for Biomedical Image Segmentation," Proc. of the 18th Int. Conf. on Medical Image Computing and Computer-Assisted Intervention (MICCAI 2015), Part 3, pp. 234-241, 2015. https://doi.org/10.1007/978-3-319-24574-4_28

[16] L. Zhang, F. Yang, Y. D. Zhang, and Y. J. Zhu, "Road Crack Detection Using Deep Convolutional Neural Network," 2016 IEEE Int. Conf. on Image Processing (ICIP), pp. 3708-3712, 2016. https://doi.org/10.1109/ICIP.2016.7533052

[17] Q. Zou, Y. Cao, Q. Li, Q. Mao, and S. Wang, "CrackTree: Automatic Crack Detection from Pavement Images," Pattern Recognition Letters, Vol.33, No.3, pp. 227-238, 2012. https://doi.org/10.1016/j.patrec.2011.11.004

[18] M. Eisenbach et al., "How to Get Pavement Distress Detection Ready for Deep Learning? A Systematic Approach," 2017 Int. Joint Conf. on Neural Networks (IJCNN), pp. 2039-2047, 2017. https://doi.org/10.1109/IJCNN.2017.7966101

[19] Y. Shi, L. Cui, Z. Qi, F. Meng, and Z. Chen, "Automatic Road Crack Detection Using Random Structured Forests," IEEE Trans. on Intelligent Transportation Systems, Vol.17, No.12, pp. 3434-3445, 2016. https://doi.org/10.1109/TITS.2016.2552248

[20] R. Amhaz, S. Chambon, J. Idier, and V. Baltazart, "Automatic Crack Detection on Two-Dimensional Pavement Images: An Algorithm Based on Minimal Path Selection," IEEE Trans. on Intelligent Transportation Systems, Vol.17, No.10, pp. 2718-2729, 2016. https://doi.org/10.1109/TITS.2015.2477675

Name:
Tomoko Aoki

Affiliation:
Japan Broadcasting Corporation

Address:
1-5-1 Chofugaoka, Chofu, Tokyo 182-8585, Japan

Brief Biographical History:
2021-2022 Graduate Student, The University of Electro-Communications
2023- Japan Broadcasting Corporation

Name:
Erika Yamamoto

Affiliation:
IBM Japan, Ltd.

Address:
1-5-1 Chofugaoka, Chofu, Tokyo 182-8585, Japan

Brief Biographical History:
2020-2021 Graduate Student, The University of Electro-Communications
2023- IBM Japan, Ltd.

Name:
Hiroshi Masuda

ORCID:
0000-0001-9521-6418

Affiliation:
Professor, The University of Electro-Communications

Address:
1-5-1 Chofugaoka, Chofu, Tokyo 182-8585, Japan

Brief Biographical History:
1987-1998 IBM Tokyo Research Laboratory
1998-2012 Associate Professor, The University of Tokyo
2013- Professor, The University of Electro-Communications

Membership in Academic Societies:
- The Japan Society for Precision Engineering (JSPE)
- The Japan Society of Mechanical Engineers (JSME)